

Regularization of material instabilities by meshfree approximations with intrinsic length scales

Jiun-Shyan Chen^{1,*†‡}, Cheng-Tang Wu^{1,§} and Ted Belytschko^{2,¶}

¹*Department of Mechanical Engineering and Center for Computer-Aided Design, The University of Iowa, Iowa City, IA 52242-1527, U.S.A.*

²*Department of Mechanical Engineering, Northwestern University, Evanston, IL 60208, U.S.A.*

SUMMARY

Meshfree approximation, such as Moving Least Square (MLS) and Reproducing Kernel (RK) approximations, possess intrinsic non-local properties. These non-local properties of meshfree approximations are exploited to incorporate an intrinsic length scale which regularizes problems with material instabilities. The discrete equilibrium equation is obtained by employing an assumed strain method in the Galerkin approximation. This proposed method is essentially uniformly non-local, but in contrast to non-local finite elements, no kinematic modes are observed. Gradient-type regularization can also be modelled by this method without the additional boundary conditions and other complications of the conventional gradient methods. Numerical examples show that the displacement-based MLS/RK formulation (1-level regularization) is sufficient to remedy mesh-sensitivity in damage-induced strain localization. For strain localization associated with plasticity, a two-level MLS/RK regularization in displacement and strain shown to be effective. Copyright © 2000 John Wiley & Sons, Ltd.

KEY WORDS: material instability; meshfree; strain localization; non-local theory; gradient method

1. INTRODUCTION

Strain localization arising from material instability poses considerable difficulties in numerical solutions, due to the loss of ellipticity in the governing equations. To remedy the loss of ellipticity, a length scale must be incorporated, implicitly or explicitly, into the material description or the formulation of the boundary value problem. For example, rate-dependent material models

* Correspondence to: Jiun-Shyan Chen, Department of Mechanical Engineering, The University of Iowa, 2133 Engineering Building, Iowa City, IA 52242-1527, U.S.A.

† E-mail: jschen@icaen.uiowa.edu

‡ Associate Professor

§ Post-Doctoral Fellow

¶ Professor

Contract/grant sponsor: National Science Foundation

Contract/grant sponsor: Office of Naval Research

introduce length scales as discussed in Reference [1]. The rate-dependent material does not lose strong ellipticity, and strain localization is caused by inhomogeneity. In strain gradient theories [2], the stress depends on strain derivatives, and these methods explicitly introduce material characteristic lengths [3]. For rate-independent materials in standard continuum theories, on the other hand, no length scale appears in the boundary value problem. In a finite element solution, the element size then serves as a length scale. As a result, finite element solutions are very sensitive to the mesh size and orientation. The strain localizes into a single element, the energy dissipation continues to decrease as the mesh is refined, and all of these non-physical properties are reflected in the mesh-sensitive load–displacement response [4].

A number of approaches have been proposed to remedy this difficulty. In non-local theory, stress at a point is related to strain in a neighbourhood. The characteristic length depends on the weight function. Some studies have also been made to justify the characteristic length in the non-local approach by microstructure [5]. The idea of a non-local continuum originally appeared in the work of Kroner *et al.* [6]. It was first applied to regularization of material instability problems using imbricate elements by Bazant *et al.* [4] and Belytschko *et al.* [7] for strain-softening materials. Non-local damage was developed by Pijaudier and Bazant [8], and several versions of non-local models based on a similar concept were later proposed by Bazant and co-workers [9, 10]. Another finite element implementation of non-local plasticity was introduced by Stromberg *et al.* [11].

An alternative procedure is to add gradients of the state variables; this approach has been used primarily in plasticity [12]. In gradient plasticity, the yield function or plastic multiplier depends on second-order spatial derivatives of effective plastic strain, which introduces a length scale. The physical motivation of gradient methods have been discussed by Aifantis [13], and a general formulation and computational algorithm for gradient plasticity was given by de Borst *et al.* [2]. Recently, de Borst *et al.* [3] has incorporated the gradient terms in a continuum damage model and applied it to 1-D quasi-brittle and frictional materials. Another type of regularization can be formulated by the micro-polar continuum [14], which was applied to strain-softening problems by Muhlhaus *et al.* [15]. In the Cosserat model, the additional degree of freedom (micro-rotation) introduces an internal length scale which prevents the strain from becoming discontinuous [16]. The computational algorithms for the elastoplastic Cosserat model was later formulated by de Borst and Sluys [17]. An alternative gradient-type approach is to add higher-order gradient terms in the governing equations, Lasry and Belytschko [18].

Localization can also be treated as a discontinuity in the displacements or strains. Ortiz *et al.* [19] proposed adding a strain discontinuity when a material instability is detected. Belytschko *et al.* [20] embedded a strain band within an element to capture strain localization. In order to account for the multiple-scale nature of strain localization, Belytschko *et al.* [21] proposed a spectral approximation superimposed on a finite element mesh to obtain higher resolution. Garikipati and Hughes [22] have discussed these problems in a multiple scale framework.

The methods mentioned above are based on weak discontinuity, i.e. a discontinuity in strain. The other approach is to consider the model with strong discontinuities, where a jump in the displacement field is considered. To overcome the problem of infinite strains caused by displacement discontinuities, a regularized softening parameter was introduced. Finite element methods based on this approach has been presented by Simo *et al.* [23], Larsson *et al.* [24], Armero *et al.* [25], and Oliver [26]. Recently, Larsson *et al.* [27] used the enhanced strain concept to embed a discontinuous displacement mode in an element.

Meshfree methods developed in recent years [28–35] share an essential feature: the approximation functions are not *locally* constructed. In the commonly used approximation theories for meshfree discretization, such as the Moving Least Square (MLS) approximation in the Element-Free Galerkin method [28, 29, 34–36] or the Reproducing Kernel (RK) approximation [30, 31, 33, 37, 38], *non-locality* is embedded in the weight function. The support size of the weight function is usually greater than the nodal spacing and therefore the approximation is inherently non-local. Two important properties can be realized in MLS and RK approximations. First, the accuracy of the approximation can be improved by enrichment; the order of the monomial basis functions determines the order of accuracy in the approximation. Second, a relationship can be established between the MLS/RK approximations and the gradient regularization method. The order of the completeness of the monomial basis functions in MLS/RK approximation can be related to the order of the gradient method. Using MLS/RK approximation with the appropriate arrangement of the reproducing conditions, a specific form of gradient regularization can be embedded in the approximation.

These approaches have an inherent advantage over the gradient method. In discretization of gradient methods, higher-order differentiable shape functions are required and additional boundary conditions are needed. The physical meaning of the additional boundary conditions is still an open issue [3]. C^1 shape functions are difficult to construct in the finite element setting, whereas in the MLS and RK approximations smooth shape functions results naturally if the weight is smooth. We also note that: (1) the enrichment of monomial basis functions in the approximation provides higher accuracy for the pre-bifurcation solution and for the solution of non-localized regions, and (2) when strain localization occurs, the non-local properties in the approximations serve as a means of regularization.

In this work, non-local displacement and strain shape functions are constructed using MLS/RK approximation. An assumed strain method is employed to formulate the discrete equations in the Galerkin framework. The paper is organized as follows: Section 2 discusses a MLS/RK non-local regularization and its relationship to the gradient method. In Section 3, the construction of strain shape functions using the MLS/RK strain smoothing regularization is presented; the Galerkin approximation using MLS/RK displacement and strain shape functions in an assumed strain variational framework is also introduced. Several quasi-static strain localization in rate-independent plasticity and continuum damage mechanics are analysed in Section 4, and a conclusion is given in Section 5.

2. MOTIVATION

The similarity of non-local theory and the meshless approximation can be inferred from a comparison of the expression for the state variables in these theories. The standard non-local form of a state variable q is given by

$$\tilde{q}(\mathbf{x}) = \int_{\Omega} W(\mathbf{x} - \mathbf{s}) q(\mathbf{s}) \, d\mathbf{s} \quad (1)$$

where \tilde{q} is the non-local state variable or a strain component corresponding to the local variable or strain component q . The variable may be a strain component ε_{ij} , an invariant of the strain

tensor, such as the trace ε_{kk} or a damage parameter d . In the above, $W(\mathbf{x})$ is a weight function that generally possesses the following properties:

$$W(\mathbf{x}) \geq 0 \quad (2)$$

$$\int_{\Omega} W(\mathbf{x}) \, d\mathbf{x} = 1 \quad (3)$$

The support of $W(\mathbf{x})$ is compact, i.e. $W(\mathbf{x} - \mathbf{s}) > 0$ only in a small neighbourhood of \mathbf{s} . $W(\mathbf{x} - \mathbf{s})$ is an even function of $\mathbf{x} - \mathbf{s}$, so that

$$\int_{\Omega} (\mathbf{x} - \mathbf{s}) W(\mathbf{x} - \mathbf{s}) \, d\mathbf{s} = 0 \quad (4)$$

The continuous form of the kernel approximation which underlies meshfree methods is given by

$$q^h(\mathbf{x}) = \int_{\Omega} w(\mathbf{x} - \mathbf{s}) q(\mathbf{s}) \, d\mathbf{s} \quad (5)$$

where $q^h(\mathbf{x})$ is the approximation of the function $q(\mathbf{x})$ and $w(\mathbf{x} - \mathbf{s})$ is the dilation function (also called the kernel window or smoothing function). It can be seen by comparing Equations (1) and (5) that the non-local variable is related to its local counterpart by equations identical to the kernel approximation if the kernel is the same as the weight function, i.e. if $w(\mathbf{x}) = W(\mathbf{x})$.

A slight difference arises between the non-local form and the kernel approximation when we consider the discrete form of Equation (5), which is used in any computation. The discretization is usually obtained by quadrature of Equation (5) in terms of coefficient q_I . This yields the following discretization of Equation (1)

$$q^h(\mathbf{x}) = \sum_I w_I(\mathbf{x}) q_I \Delta\Omega_I \quad (6)$$

where $w_I(\mathbf{x}) \equiv w(\mathbf{x} - \mathbf{x}_I)$ is the weight function of node I and $\Delta\Omega_I$ is the volume (or area) associated with node I .

For an arbitrary weight function, the above does not yield a convergent discretization. For convergence in second-order partial differential equations, it is necessary that the approximation satisfy the reproducing conditions for linear polynomials (which are equivalent to the conditions of linear polynomial completeness, often called consistency). These conditions for an approximation function $\Phi_I(\mathbf{x})$ are

$$\sum_I \Phi_I(\mathbf{x}) = 1 \quad (7a)$$

$$\sum_I \Phi_I(\mathbf{x}) x_{iI} = x_i \quad (7b)$$

The above can be satisfied by modifying the weight $w_I(\mathbf{x})$ in Equation (6) by a correction function of Liu and Chen [32], or by developing the approximation from a Moving Least Square (MLS) of Belytschko *et al.* [28]. In either case, the approximation functions are related to the weight functions by

$$\Phi_I(\mathbf{x}) = [\alpha_0(\mathbf{x}) + \alpha_1(\mathbf{x})(x - x_I) + \alpha_2(\mathbf{x})(y - y_I)] w_I(\mathbf{x}) \quad (8)$$

and the approximations are identical. The relationship between the non-local method and a gradient regularization can be illustrated by taking a Taylor series of the variable $q(\mathbf{s})$ in Equation (5):

$$q(\mathbf{s}) = q(\mathbf{x}) + q_{,i}(\mathbf{x})(s_i - x_i) + \frac{1}{2} q_{,ij}(\mathbf{x})(s_i - x_i)(s_j - x_j) + O(\|\mathbf{x} - \mathbf{s}\|^3) \quad (9)$$

Substituting Equation (9) into Equation (1) gives

$$\begin{aligned} \tilde{q}(\mathbf{x}) &= q(\mathbf{x}) \int_{\Omega} W(\mathbf{x} - \mathbf{s}) \, ds \\ &\quad + q_{,i}(\mathbf{x}) \int_{\Omega} (s_i - x_i) W(\mathbf{x} - \mathbf{s}) \, ds \\ &\quad + \frac{1}{2} q_{,ij}(\mathbf{x}) \int_{\Omega} (s_i - x_i)(s_j - x_j) W(\mathbf{x} - \mathbf{s}) \, ds + O(\|\mathbf{x} - \mathbf{s}\|^3) \\ &= q(\mathbf{x}) + \frac{1}{2} q_{,ij}(\mathbf{x}) m_{ij} \end{aligned} \quad (10)$$

where we have used Equations (3), (4) and the definition

$$m_{ij} = \int_{\Omega} (s_i - x_i)(s_j - x_j) W(\mathbf{x} - \mathbf{s}) \, ds \quad (11)$$

In one dimension, Equation (10) becomes

$$\tilde{q}(x) = q(x) + \frac{m_{xx}}{2} q(x)_{,xx} \quad (12)$$

So the non-local model under the standard assumption on the weight function is equivalent to a gradient theory. The non-local model is identical to the continuous form of the meshless kernel approximation, according to Equations (1) and (5). Therefore a kernel approximation is basically identical to both a non-local model and a gradient model.

The one gap that remains is between the discrete kernel approximation and the gradient method. There are two steps from the continuous kernel approximation Equation (5) to the discrete kernel approximation:

- (i) The discretization of Equation (5) by quadrature of the right-hand side, i.e., the step to Equation (6).
- (ii) The correction of the approximation of Equation (6) so that the reproducing conditions in Equation (7) are met. The correction of the approximation will be discussed in the next section.

The effect of these can be ascertained readily by a Fourier analysis, which will be published elsewhere.

3. DISCRETIZATION

We have found by numerical studies that sometimes it does not suffice to use a non-local approximation of the displacement to replicate a gradient theory. Instead, it is necessary to

approximate the non-local variable directly. For this purpose, we use a multi-field weak form. The assumed strain method is used, so the non-local strain is approximated directly in terms of the displacement parameters. In order to obtain a non-local approximation, it is necessary to use a larger window for the strain approximation.

Since in the assumed strain method, the strain is approximated directly, it is convenient to use kernels which satisfy the reproducing conditions developed by Li and Liu [39, 40]. We illustrate this in one dimension. The displacement field is first approximated by the discrete form of corrected kernel approximation:

$$u^h(x) = \sum_{I=1}^{\text{NP}} \bar{w}_a^{[m]}(x; x - x_I) d_I \quad (13)$$

where NP is the number of nodes in the model, and $\bar{w}_a^{[m]}(x; x - x_I)$ is the corrected kernel (or weight function) with dilation a ; the dilation is equivalent to the support of the weight function. The superscript m on the kernel refers to the order of polynomial that can be reproduced by Equation (13). The corrected weight function is given by a generalization of Equation (8):

$$\bar{w}_a^{[m]}(x; x - x_I) = [a_0(x) + a_1(x)(x - x_I) + \cdots + a_m(x)(x - x_I)^m] w_a(x - x_I) \quad (14)$$

The coefficients $a_i(x)$ are obtained from the reproducing conditions (7), which in general are

$$\sum_{I=1}^{\text{NP}} \bar{w}_a^{[m]}(x; x - x_I) x_I^p = x^p \quad \text{for } p = 0, \dots, m \quad (15)$$

Equation (15) provides $m + 1$ equations for $m + 1$ unknowns $a_i(x)$. The resulting corrected kernel is

$$\bar{w}_a^{[m]}(x; x - x_I) = \mathbf{H}^{[m]\Gamma}(0) \mathbf{M}^{[m]^{-1}}(x) \mathbf{H}^{[m]}(x - x_I) w_a(x - x_I) \quad (16)$$

$$\mathbf{M}^{[m]}(x) = \sum_{I=1}^{\text{NP}} \mathbf{H}^{[m]}(x - x_I) \mathbf{H}^{[m]\Gamma}(x - x_I) w_a(x - x_I) \quad (17)$$

Equation (13) can be rewritten in the standard form:

$$u^h(x) = \sum_{I=1}^{\text{NP}} \Psi_I^{[m]}(x) d_I \quad (18)$$

where $\Psi_I^{[m]}(x)$ are the displacement shape functions, which are given by

$$\Psi_I^{[m]}(x) = \mathbf{H}^{[m]\Gamma}(0) \mathbf{M}^{[m]^{-1}}(x) \mathbf{H}^{[m]}(x - x_I) w_a(x - x_I) \quad (19)$$

In the assumed strain method proposed here, the one-dimensional non-local strain is approximated by

$$\tilde{\varepsilon}(x) = \int_{\Omega} \bar{w}_b^{[m]}(x; x - s) \frac{du(s)}{ds} ds \quad (20)$$

where the dilation $b > a$, and $\bar{w}_b^{[m]}$ satisfies n th order reproducing conditions similar to Equation (15).

It should be noted that the reproducing condition for a continuous non-local strain form, Equation (20), leads to a similar corrected weight function, Equation (16), except that the moment matrix Equation (17) is expressed in integral form. If a discrete form of the non-local strain is used,

then the corrected weight function for non-local strain weight function, $\bar{w}_b^{[n]}$, can be obtained with the procedures in Equations (14)–(16).

For illustration, we examine the continuous expression for non-local strain. Introducing the displacement approximation Equation (18) into Equation (20) yields

$$\begin{aligned} \tilde{\varepsilon}^h(x) &= \int_{\Omega} \left(\sum_{I=1}^{NP} \frac{\partial \Psi_I^{[m]}(s)}{\partial s} d_I \right) \bar{w}_b^{[n]}(x; x - s) ds \\ &= \sum_{I=1}^{NP} \left[\int_{\Omega} \frac{\partial \Psi_I^{[m]}(s)}{\partial s} \bar{w}_b^{[n]}(x; x - s) ds \right] d_I \\ &\equiv \sum_{I=1}^{NP} \tilde{\mathbf{B}}_I(x) d_I \end{aligned} \tag{21}$$

where $\tilde{\mathbf{B}}_I(x)$ is the strain–displacement relationship for the non-local strain:

$$\tilde{\mathbf{B}}_I(x) = \int_{\Omega} \frac{\partial \Psi_I^{[m]}(s)}{\partial s} \bar{w}_b^{[n]}(x; x - s) ds \tag{22}$$

Using the reproducing conditions presented in Equation (7), with the 0th order moment of $\bar{w}_b^{[n]}$ equal to one and the first-order moment of $\bar{w}_b^{[n]}$ equal to zero, the non-local strain approximation of Equation (22) corresponds the following gradient strain:

$$\tilde{\varepsilon}^h(x) = \varepsilon^h(x) + \frac{\bar{m}_2}{2} \varepsilon_{,xx}^h(x) \tag{23}$$

$$\bar{m}_i(x) = \int_{\Omega} (x - s)^i \bar{w}_b^{[n]}(x; x - s) ds \tag{24}$$

Note that the reproducing conditions $\bar{m}_0 = 1, \bar{m}_1 = 0$ needed for Equation (23) require linear basis functions in $\bar{w}_b^{[n]}$, i.e. $n = 1$ and $w_b^{[1]}(x; x - s) = [a_0(x) + a_1(x)(x - s)]w_b(x - s)$. The two coefficients, $a_0(x)$ and $a_1(x)$, are obtained by solving Equation (7). Similar procedures can be used to obtain higher-order gradient models with higher-order reproducing conditions. In two-dimensions, the non-local strain is

$$\tilde{\boldsymbol{\varepsilon}}^h(\mathbf{x}) = \sum_{I=1}^{NP} \tilde{\mathbf{B}}_I(\mathbf{x}) \mathbf{d}_I \tag{25}$$

where $\tilde{\boldsymbol{\varepsilon}}^{h^T} = [\tilde{\varepsilon}_{11}^h, \tilde{\varepsilon}_{22}^h, 2\tilde{\varepsilon}_{12}^h]$, $\mathbf{d}_I^T = [d_{1I}, d_{2I}]$ and $\tilde{\mathbf{B}}_I(\mathbf{x})$ is the assumed strain matrix for the gradient (non-local) strain. The matrix is given by

$$\tilde{\mathbf{B}}_I(\mathbf{x}) = \begin{bmatrix} \tilde{\mathcal{G}}_{1I}(\mathbf{x}) & 0 \\ 0 & \tilde{\mathcal{G}}_{2I}(\mathbf{x}) \\ \tilde{\mathcal{G}}_{2I}(\mathbf{x}) & \tilde{\mathcal{G}}_{1I}(\mathbf{x}) \end{bmatrix} \tag{26}$$

where

$$\tilde{\mathcal{G}}_{iI}(\mathbf{x}) = \int_{\Omega} \mathcal{G}_{iI}(\mathbf{s}) \bar{w}_b^{[n]}(\mathbf{x}, \mathbf{s}) ds = \int_{\Omega} \frac{\partial \Psi_I^{[m]}(\mathbf{s})}{\partial s_i} \bar{w}_b^{[n]}(\mathbf{x}, \mathbf{s}) ds \tag{27}$$

To introduce the gradient strain into the Galerkin approximation, we use the weak form:

$$\delta\Pi(\tilde{\boldsymbol{\varepsilon}}, \mathbf{u}) = \int_{\Omega} \delta\tilde{\boldsymbol{\varepsilon}}^T \boldsymbol{\tau}(\tilde{\boldsymbol{\varepsilon}}) \, d\mathbf{x} - \delta W^{\text{ext}}(\mathbf{u}) = 0 \quad (28)$$

where $\boldsymbol{\tau}$ is the stress computed from the assumed non-local strain $\tilde{\boldsymbol{\varepsilon}}$. By introducing displacement and strain shape functions, and using the mixed transformation method to impose essential boundary conditions [41], the discrete equations are obtained:

$$\mathbf{f}^{\text{int}} = \boldsymbol{\Lambda}^{-T} \int_{\Omega_x} \tilde{\mathbf{B}} \boldsymbol{\tau}(\tilde{\boldsymbol{\varepsilon}}) \, d\mathbf{x} = \mathbf{f}^{\text{ext}} \quad (29)$$

The linearization of Equation (29) is

$$\mathcal{H} \Delta \mathbf{d} = \Delta \not\phi \quad (30)$$

where

$$\mathcal{H} = \boldsymbol{\Lambda}^{-T} \tilde{\mathbf{K}} \quad (31)$$

$$\Delta \not\phi = \mathbf{f}^{\text{ext}} - \mathbf{f}^{\text{int}} \quad (32)$$

$$\tilde{\mathbf{K}}_{JJ} = \int_{\Omega_x} \tilde{\mathbf{B}}_J^T \mathbf{C} \tilde{\mathbf{B}}_J \, d\mathbf{x} \quad (33)$$

where $\boldsymbol{\Lambda}$ is the transformation matrix between generalized and nodal co-ordinates according to [41] for the purpose of imposing boundary conditions, \mathbf{C} is the material response matrix, and \mathbf{f}^{ext} is the discrete external force.

4. EXAMPLES

The following examples illustrate the regularization of the rate-independent models with material instabilities using the proposed method, and the relationship to the gradient theories is also studied. Strain localization induced by elastic damage and plasticity is considered. A continuum damage theory based on the thermodynamics of irreversible process and internal state variable theory [42] is used with a strain-based isotropic damage function [43]. The plasticity model is based on the J_2 flow rule with softening.

4.1. Matching between the reproducing kernel regularization and the gradient method in a one-dimensional elastic-damage problem

Although the proposed regularization is non-local, the method can be tailored to provide a regularization similar to that of finite element gradient type methods; this follows from the equivalence described in Section 2. To verify this concept, we match the gradient solution by Peerlings *et al.* [44] with the proposed MLS/RK strain regularization in an elastic-damage problem. In Peerlings *et al.* [44], the strain-based damage evolution equations are

$$\boldsymbol{\sigma} = (1 - D) E \boldsymbol{\varepsilon} \quad (34)$$

$$\dot{\boldsymbol{\sigma}} = (1 - D) E \dot{\boldsymbol{\varepsilon}} - E \boldsymbol{\varepsilon} \dot{D} \quad (35)$$

$$\dot{D} = \begin{cases} 0 & \text{if } \tilde{\varepsilon}_{\text{eq}} < k \\ \frac{\partial D}{\partial k} \dot{\tilde{\varepsilon}}_{\text{eq}} & \text{otherwise} \end{cases} \quad (36a)$$

$$\quad (36b)$$

where $0 \leq D \leq 1$ is the damage parameter and k is the damage threshold. Peerlings *et al.* [44] introduces the following regularization on the equivalent strain:

$$\tilde{\varepsilon}_{\text{eq}} = \varepsilon_{\text{eq}} + c \nabla^2 \varepsilon_{\text{eq}} \quad (37)$$

where $\tilde{\varepsilon}_{\text{eq}}$ is the regularized equivalent strain, ε_{eq} is the local equivalent strain computed from the displacements, and c is the regularization parameter. Since the weak form of Equation (37) requires C^1 continuity in the displacements, the non-local character was implemented [44] by solving

$$\tilde{\varepsilon}_{\text{eq}} - c \nabla^2 \tilde{\varepsilon}_{\text{eq}} = \varepsilon_{\text{eq}} \quad (38)$$

If $\tilde{\varepsilon}_{\text{eq}}$ is treated as an independent variable, the discrete form of Equation (38) requires only a C^0 interpolation for displacements and $\tilde{\varepsilon}_{\text{eq}}$. One major difficulty in the theory of [44] is that additional boundary conditions are required for the strains, and no physical basis for such boundary conditions is available.

It should be noted that in [44], the gradient theory is only introduced in the equivalent strain involved in the damage evolution equations. Therefore, in our comparison, the non-local MLS/RK approximation (strain smoothing) is only applied to the equivalent strains. The following approximation is used

$$\tilde{\varepsilon}_{\text{eq}}(x) = \int_{\Omega} \varepsilon_{\text{eq}}(s) \bar{w}_b^{[n]}(x; x-s) ds \quad (39)$$

$$\bar{w}_b^{[n]}(x; x-s) = \mathbf{H}^{[n]\top}(0) \mathbf{M}^{[n-1]}(x) \mathbf{H}^{[n]}(x-s) w_b(x-s) \quad (40a)$$

with $n = 1$, $H^{[1]\top}(x) = [1, x]$. By expressing

$$\varepsilon_{\text{eq}}(s) = \varepsilon_{\text{eq}}(x) + \sum_{i=1}^{\infty} \frac{(-1)^i}{i!} (x-s)^i \partial^i \varepsilon_{\text{eq}}(x) / \partial x^i \quad (40b)$$

in Equation (39) and using $\int_{\Omega} \bar{w}_b^{[1]}(x; x-s) ds = 1$ and $\int_{\Omega} (x-s) \bar{w}_b^{[1]}(x; x-s) ds = 0$, one can relate the MLS/RK strain smoothing to the gradient method by

$$\tilde{\varepsilon}_{\text{eq}}(x) = \varepsilon_{\text{eq}}(x) + \frac{1}{2!} \bar{m}_2(x) \varepsilon_{\text{eq},xx}(x) + \text{higher-order terms} \quad (41)$$

$$\bar{m}_2(x) = \int_{\Omega} (x-s)^2 \bar{w}_b^{[1]}(x; x-s) ds \quad (42)$$

Comparing Equations (37) and (41), we can see that the MLS/RK regularization and gradient method are related by

$$\int_{\Omega} (x-s)^2 \bar{w}_b^{[1]}(x; x-s) ds = 2c \quad (43)$$

The condition in Equation (43) provides a relation between the support size b of the weight function and the coefficient c in the gradient method.

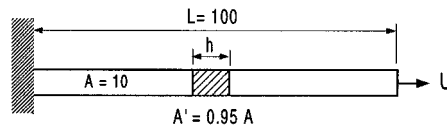


Figure 1. One-dimensional rod model.

Table I. Regularization parameters for gradient method and MLS/RK regularization (Equation (43)).

Gradient method c	0.63	1.47	2.61
MLS/RK regularization b	8	12	16

Note that (1) to match the gradient method in [44], the MLS/RK nonlocal strain is only applied to equivalent strain $\bar{\varepsilon}_{\text{eq}}$ in Equation (36); (2) the strain ε in Equation (35) is a local variable that is computed using the standard displacement shape function.

The example consists of a rod subjected to uniaxial tensile load by displacement control as shown in Figure 1. The dimensionless material constants is $E = 2 \times 10^6$, and the initial and critical values of the damage threshold k are 0.0001 and 0.00625, respectively, for the damage law used in Reference [44]. An imperfection in the cross sectional area is introduced between $x = 45$ to $x = 55$ to trigger bifurcation from a homogeneous state. The material instability due to damage will localize the deformation. A uniform 50-node mesh is employed for the meshfree and finite element computations with a gradient method. Three sets of equivalent regularization parameters based on Equation (43) are shown in Table I. The damage parameter (D), load–displacement response, and the strain predicted by the two methods are shown in Figures 2–4 for three sets of matching parameters. The results agree very closely.

This example shows that MLS/RK strain approximation with an intrinsic length scale can match a gradient theory. It avoids the higher-order gradient terms and the additional boundary conditions in the gradient approach. By choosing the support of the weight function according to (43), the gradient theory is replicated.

4.2. Elastic damage in tensile specimen with symmetric imperfection

A rectangular specimen is subjected to uniform displacements at the two ends. In order to trigger localization from a homogeneous state of deformation, symmetric material imperfections with weakened material properties are introduced as shown in Figure 5 (shaded area). In two dimensions, the elastic damage law is

$$\boldsymbol{\sigma} = (1 - D) \mathbf{C} \boldsymbol{\varepsilon} \quad (44)$$

$$D(\bar{\varepsilon}) = \begin{cases} \frac{\bar{\varepsilon}_c(\bar{\varepsilon} - \bar{\varepsilon}_i)}{\bar{\varepsilon}(\bar{\varepsilon}_c - \bar{\varepsilon}_i)} & \text{if } \bar{\varepsilon}_i \leq \bar{\varepsilon} \leq \bar{\varepsilon}_c \\ 1 & \text{if } \bar{\varepsilon}_c < \bar{\varepsilon} \end{cases} \quad (45)$$

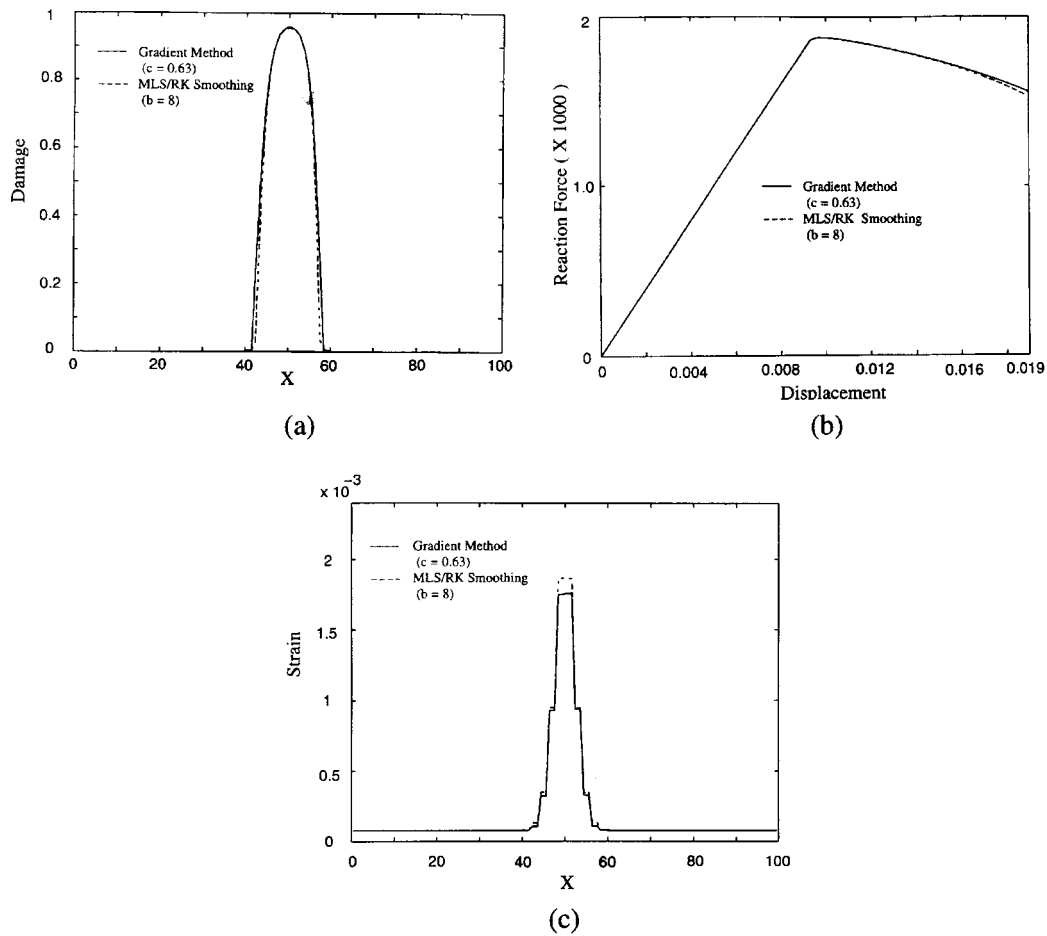


Figure 2. Comparison of damage distribution, load–displacement response, and strain distribution using gradient method ($c = 0.63$) and MLS/RK regularization ($b = 8$).

where \mathbf{C} is the elastic tensor, and $\bar{\epsilon}$ is an equivalent strain. The dimensionless material properties of the specimen are $E = 2 \times 10^6$, $\nu = 0.18$, $\bar{\epsilon}_i = 10^{-4}$, $\bar{\epsilon}_c = 6.25 \times 10^{-3}$. Three finite element meshes with different levels of refinement are used. The same nodes are used in meshfree and finite element computations.

Two meshfree formulations are considered in this study. The first method is the conventional displacement based meshfree formulation, where the MLS/RK displacement shape function is constructed based on a cubic B-spline kernel with linear basis functions ($m = 1$ in Equation (19)). We call this approach a meshfree method with one-level regularization. The second method is the meshfree formulation based on an assumed strain approximation described in Section 3. The strain shape function is constructed by the MLS/RK regularization with a normalized cubic B-spline kernel ($n = 0$ in Equation (21)) with a support size chosen to match a non-local theory.

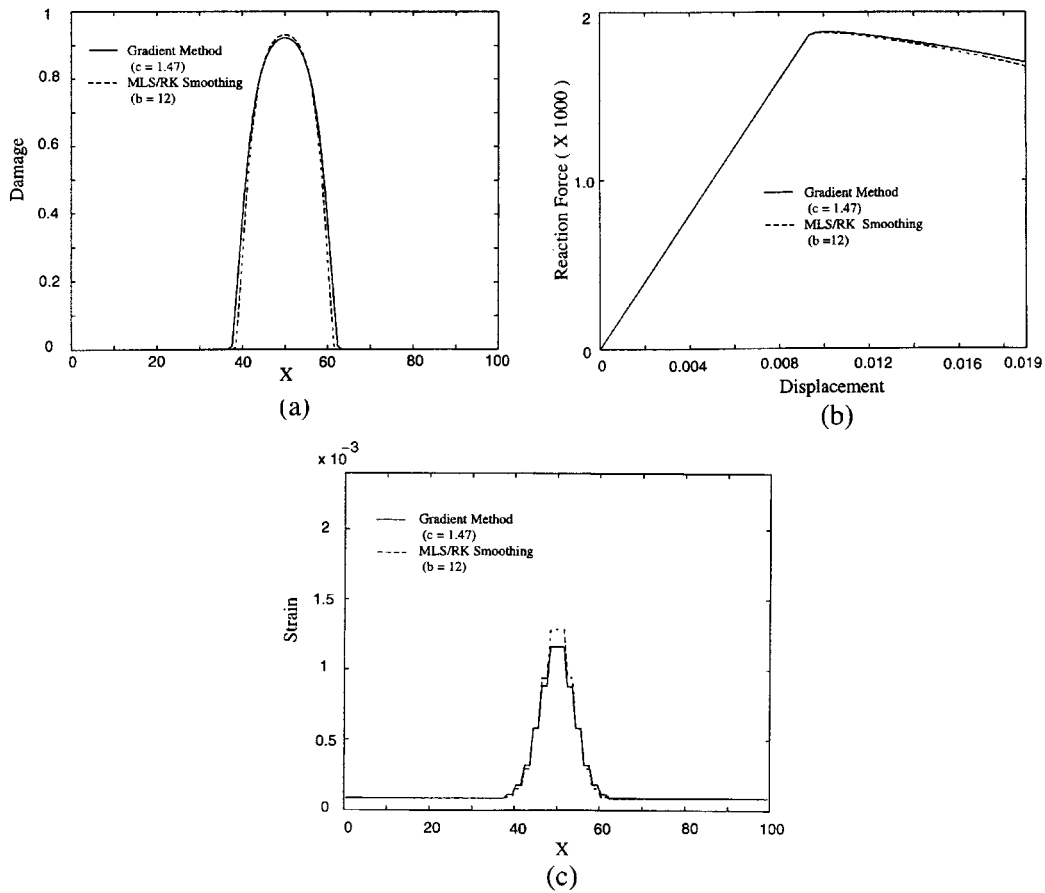


Figure 3. Comparison of damage distribution, load–displacement response, and strain distribution using gradient method ($c = 1.47$) and MLS/RK regularization ($b = 12$).

We classify this method as a meshfree method with two-level regularization. The support size of the MLS/RK displacement shape functions in all three discretizations is the nodal distance in the coarsest models in the axial direction.

Figure 6 demonstrates how the strain always localizes into one element in a finite element solution. A typical finite element load–displacement response is also presented in Figure 7; note the sensitivity to element size. The meshfree computation, on the other hand, provides a converged solution in all three models. We observe in Figure 8 that the bandwidth of intense deformation stays constant in the specimen. Due to the constant energy dissipation in the strain localization zone in the meshfree computation, the load–displacement solutions of the three models are approximately the same, as shown in Figure 9. Interestingly, in this problem, the conventional meshfree method with one-level regularization is sufficient to eliminate grid sensitivity. The meshfree solutions with one-level and two-level regularization predict almost identical results.

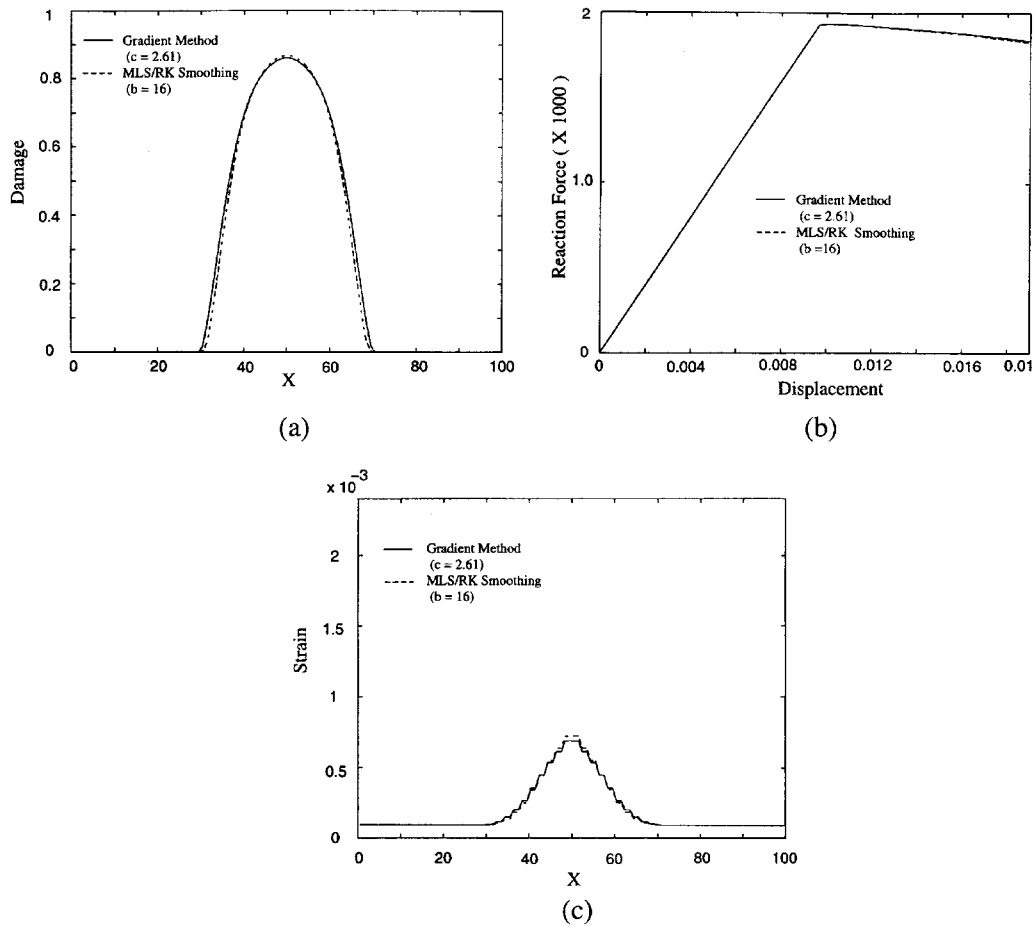


Figure 4. Comparison of damage distribution, load–displacement response, and strain distribution using gradient method ($c = 2.61$) and MLS/RK regularization ($b = 16$).

4.3. Elastic damage in tensile specimen with a symmetric imperfection

To study shear band formation, an asymmetric imperfection (shaded area) is introduced as shown in Figure 10. In this case, a coarse model and a refined model are used to examine the grid sensitivity of the proposed regularization method. We also use an unstructured model with irregular nodal spacing to investigate the sensitivity of numerical solution to nodal spacing irregularity. The boundary conditions, material properties, and MLS/RK shape functions for this problem are the same as those used in problem 4.2, except $\nu = 0.3$. The support size of the MLS/RK shape function is 1.5 times the nodal distance of the coarse regular model.

Shear band formation is clearly evident in the coarse model presented in Figure 11(a). As the model is refined, the width of the shear band stays approximately unchanged as shown in

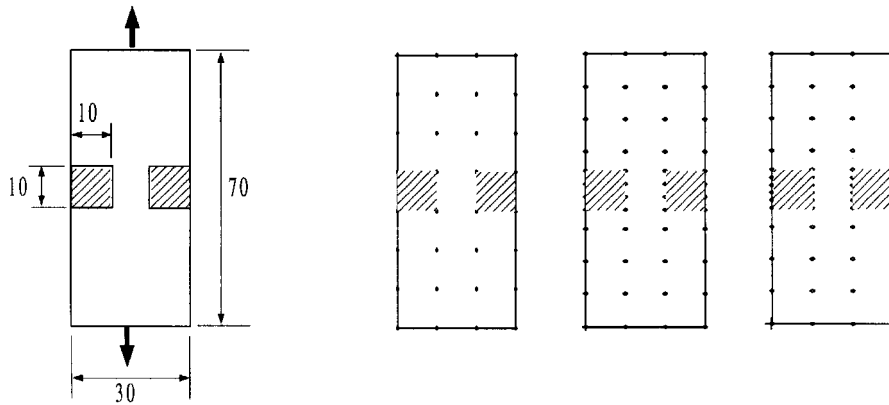


Figure 5. Elastic damage test specimen with symmetric imperfection and analysis models.

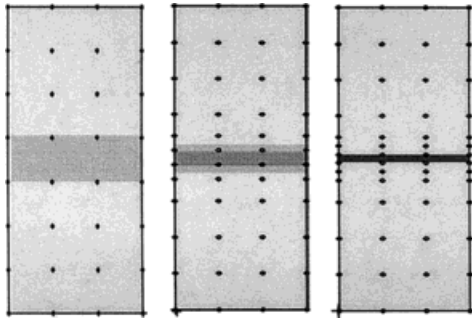


Figure 6. Finite element strain localization in elastic damage.

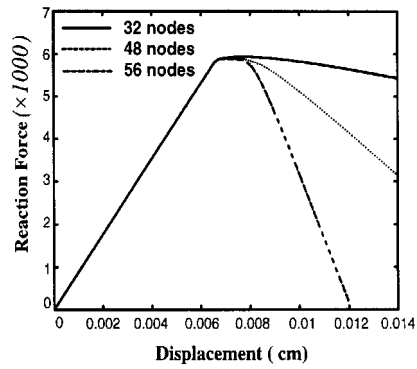


Figure 7. Finite element load-displacement curves of elastic damage.

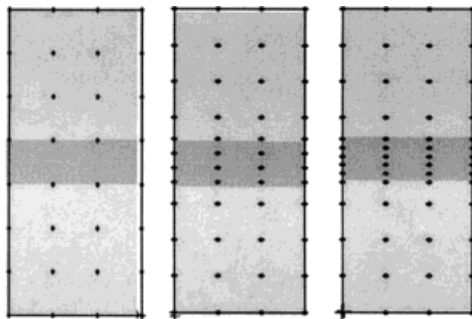


Figure 8. Strain localization of an elastic damage using MLS/RK regularization.

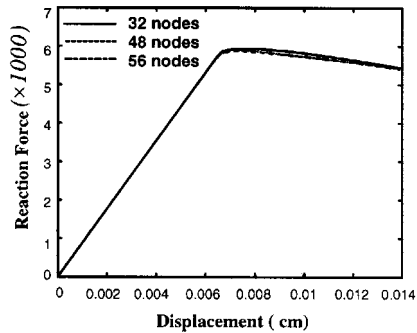


Figure 9. Load-displacement curves of an elastic damage predicted by MLS/RK regularization.

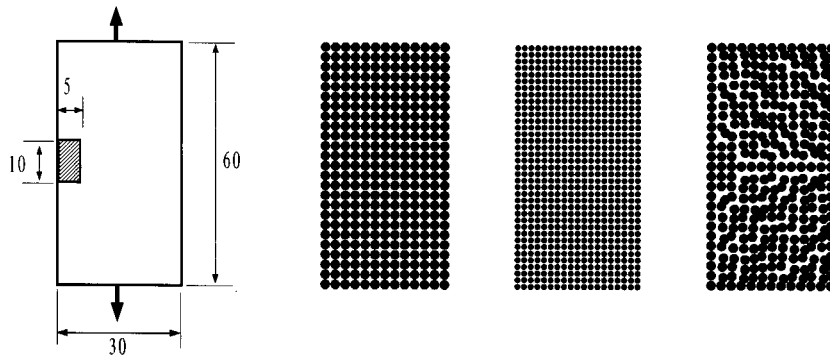


Figure 10. Elastic damage test specimen with asymmetric imperfection and analysis models.

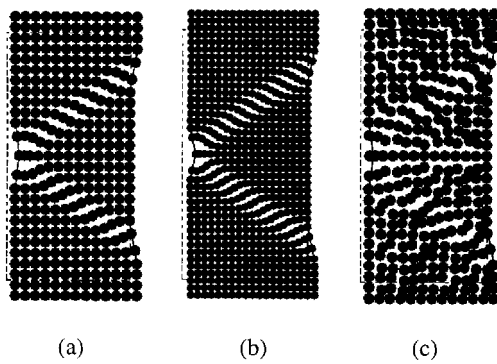


Figure 11. Elastic damage shear band localization predicted by MLS/RK regularization.

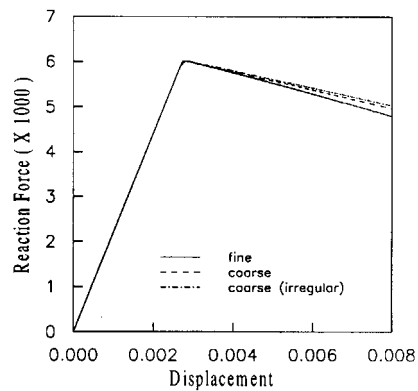


Figure 12. Load-displacement curves by MLS/RK regularization in elastic damage localization.

Figure 11(b). The irregular model also displays a shear band with a similar bandwidth; see Figure 11(c). The load-displacement curves in Figure 12 show that the meshfree solution is insensitive to both nodal refinement and irregular nodal spacing. As in the previous example, the meshfree solution with one-level regularization is almost identical to the two-level regularization solution.

4.4. Strain localization in plasticity

The previous examples demonstrate that the meshfree solution using one- and two-level regularization converge quite rapidly in problems with material instability due to damage. For plastic strain localization, however, ductility is more pronounced. This example examines whether the nonlocality in one-level regularization is sufficient to resolve grid sensitivity in plastic strain localization. The geometry of the test problem is given in Figure 13 where the shaded area again represents a weakened material. Three model refinements were used to study the regularization of

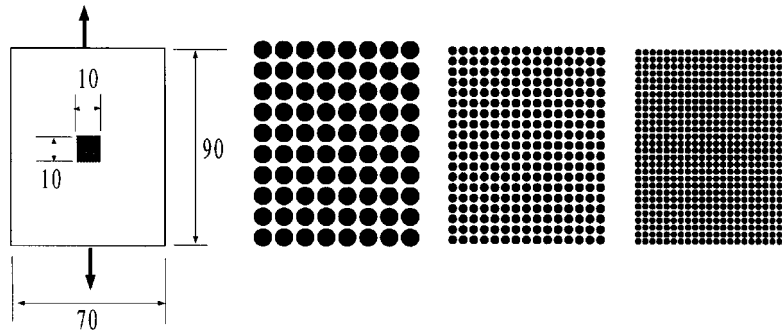


Figure 13. Problem description and analysis model of plasticity model.

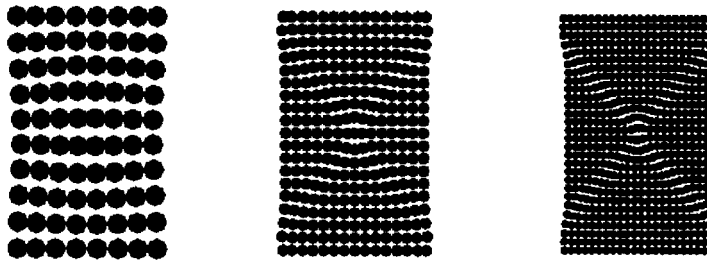


Figure 14. Plasticity strain localization using one-level MLS/RK regularization.

an approximation with an intrinsic length scale. The analysis is performed with a displacement control. The material properties are $E = 2 \times 10^6$, $\nu = 0.18$, $\sigma_y = 1.5 \times 10^4$, and the softening modulus $H = -1.2 \times 10^4$.

In this study, one- and two-level regularizations are used. The displacement and strain shape functions are constructed using a cubic B-spline kernel, with linear and constant basis functions ($m = 1$ in Equation (19) and $n = 0$ in Equation (20)), respectively. The support size in the displacement and strain shape functions are 1.5 the nodal distance of the coarsest model; 4×4 quadrature is used for the stiffness matrix and force vector, and 2×2 quadrature is employed in constructing the strain shape function.

The meshfree method with one-level regularization is studied first. The shear band results shown in Figure 14 demonstrates that the meshfree method with one-level regularization is still grid sensitive: the shear bandwidth decreases as the model is refined. This grid sensitivity in model refinement is clearly evident in the load–displacement curves in Figure 15. Using the two-level regularization method, the results improves as shown in Figure 16, although the shear band is not very visible in the coarsest case. In Figure 17, a significant improvement in the load–displacement response using the two-level regularization is observed compared to that for one-level regularization.

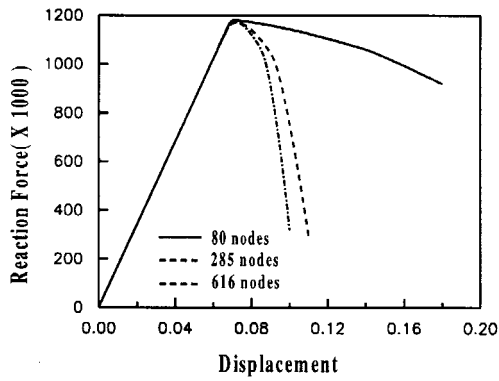


Figure 15. Plasticity load–displacement curves obtained by one-level MLS/RK regularization.

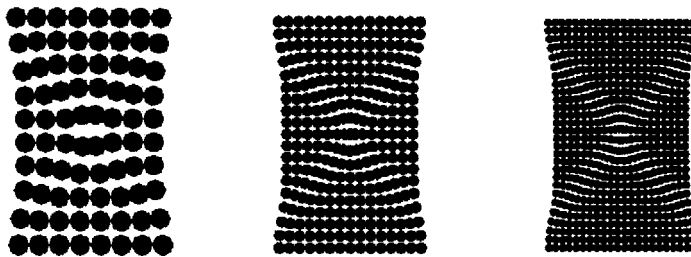


Figure 16. Plastic strain localization using two-level MLS/RK regularization.

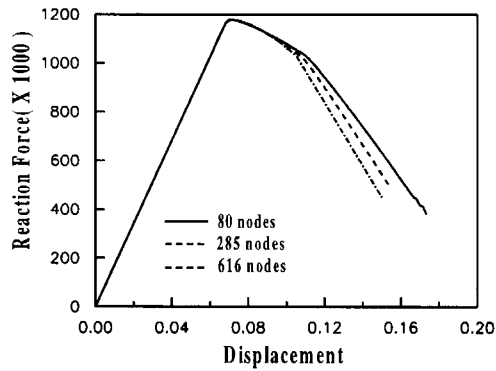


Figure 17. Plasticity load–displacement curves obtained by two-level MLS/RK regularization.

5. CONCLUSION

We have demonstrated that a length scale can be directly incorporated into a meshfree approximation to regularize problems with material instabilities. The resulting regularization can duplicate results obtained with gradient regularization. We have shown also a relationship to non-local theories, so it is anticipated that the methodology will be applicable to non-local regularizations. The length scale is introduced implicitly in the construction of the approximation, and can be considered an intrinsic length scale since it resides in the approximation but is independent of the degree of discretization refinement. A major advantage of these methods is that they do not entail any additional boundary conditions, such as commonly found in gradient regularization. They also appear to be highly robust.

The implicit length scale has been incorporated in a meshfree approximation. The method was motivated by the similarity of the continuous form of the meshfree approximation and the non-local representation of a variable. Meshfree approximations are ideally suited for such implicit non-local approximations since the length scale can be embedded in the approximation by appropriately setting the size of the window function. It has been shown that the parameters of a gradient approximation of a state variable or strain are related to the window size and the order of completeness of the meshfree approximation. Such techniques could also be implemented in finite element methods, but they would not be as natural.

Two types of implicit length scale implementations have been described. In the first, called one-level regularization, the length scale is only incorporated in the displacement approximation. This type of approximation is relatively successful in some problems, but fails when applied to softening plasticity. In the second, which is called two-level regularization, the length scale is embedded in the strain approximation. For this purpose, an assumed strain method is used. This methodology provides an almost perfect match with the results of a gradient regularization.

The application of the methodology is illustrated in several problems, both one dimensional and two dimensional. In the first example, the intrinsic length scale approximation is embedded in the strain approximation; a damage model is used for the material. Almost perfect agreement is achieved with a gradient method results. The second and third examples demonstrate that the mesh sensitivity difficulties are successfully eliminated by both one-level and two-level regularizations. It is shown in the last example that a two-level regularization is needed to obtain convergent solution in strain softening plasticity.

The simplicity of this approach to regularization of problems with material instabilities makes it very attractive. It should be possible to easily extend this methodology to problems with multiple length scales. Several theoretical questions, such as the exact effects of the discretization on the intrinsic length scale, remain to be resolved and are addressed in another paper.

ACKNOWLEDGEMENT

The support of this research by the National Science Foundation to the University of Iowa and the Office of Naval Research to Northwestern University is greatly acknowledged.

REFERENCES

1. Needleman A. Material rate dependence and mesh sensitivity in localization problems. *Computer Methods in Applied Mechanics and Engineering* 1987; **67**:68–85.

2. de Borst R, Muhlhaus HB. Gradient-dependent plasticity: formulation and algorithmic aspects. *International Journal for Numerical Methods in Engineering* 1992; **35**:521–539.
3. de Borst R, Pamin RH, Peerlings RHJ, Sluys LJ. On gradients-enhanced damage and plasticity models for failure in quasi-brittle and frictional materials. *Computational Mechanics* 1995; **17**:130–141.
4. Bazant ZP, Belytschko T, Chang T-P. Continuum model for strain softening. *Journal of Engineering Mechanics* 1984; **110**:1666–1692.
5. Bazant ZP, Pijaudier-Cabot G. Measurement of the characteristic length of nonlocal continuum. *ASME Journal of Engineering Mechanics* 1989; **113**:2333–2347.
6. Kroner E. Elasticity theory of materials with long-range cohesive forces. *International Journal of Solids and Structures* 1967; **3**:731–742.
7. Belytschko T, Bazant ZP, Hyun Y-W, Chang T-P. Strain-softening materials and finite-element solutions. *Computers and Structures* 1986; **23**:163–180.
8. Pijaudier-Cabot G, Bazant ZP. Nonlocal damage theory. *Journal of Engineering Mechanics* 1987; **113**:1512–1533.
9. Bazant ZP, Lin F-B. Nonlocal yield limit degradation. *International Journal for Numerical Methods in Engineering* 1988; **26**:1805–1823.
10. Bazant ZP, Ozbolt J. Nonlocal microplane model for fracture, damage and size effect in structure. *Journal of Engineering Mechanics* 1990; **116**:2482–2504.
11. Stromberg L, Ristinmaa M. FE-formulation of a nonlocal plasticity theory. *Computer Methods in Applied Mechanics and Engineering* 1996; **136**:127–144.
12. Comi C, Perego U. A generalized variable formulation for gradient dependent softening plasticity. *International Journal for Numerical Methods in Engineering* 1996; **39**:3731–3755.
13. Aifantis EC. The physics of plastic deformation. *International Journal of Plasticity* 1987; **3**:211–247.
14. Cosserat E, Cosserat F. *Theorie des corps deformables*. Paris: Herman, 1909.
15. Muhlhaus HB, Vardoulakis L. The thickness of shear bands in granular materials. *Geotechnique* 1987; **37**: 271–283.
16. Steinmann P, Willam K. Localization in micropolar elasto-plasticity. In *Proceedings of the Third International Conference on Constitutive Equations for Engineering Material*. Desai CS et al. (eds). ASME, New York, 1991; 461–465.
17. de Borst R, Sluys LJ. Localization in a Cosserat continuum under static and loading conditions. *Computer Methods in Applied Mechanics and Engineering* 1991; **90**:805–827.
18. Larys D, Belytschko T. Localization limiters in transient problems. *International Journal of Solids and Structures* 1988; **24**:581–597.
19. Ortiz M, Leroy Y, Needleman A. A finite element method for localized failure analysis. *Computer Methods in Applied Mechanics and Engineering* 1987; **61**:189–214.
20. Belytschko T, Fish J, Englemann B. A finite element method with embedded-localization zones. *Computer Methods in Applied Mechanics and Engineering* 1988; **70**:59–90.
21. Belytschko T, Fish J, Bayliss A. The spectral overlay on finite elements for problems with high gradients. *Computer Methods in Applied Mechanics and Engineering* 1990; **81**:71–89.
22. Garikipati K, Hughes TJR. A study of strain localization in a multiple scale framework—The one-dimensional problem. *Computer Methods in Applied Mechanics and Engineering* 1998; **159**:193–222.
23. Simo JC, Oliver J, Armero F. An analysis of strong discontinuities induced by strain-softening in rate-independent solids. *Computational Mechanics* 1993; **12**:277–296.
24. Larsson R, Runesson K, Ottosen NS. Discontinuous displacement approximation for capturing plastic localization. *International Journal for Numerical Methods in Engineering* 1993; **36**:2087–2105.
25. Armero F, Garikipati K. Recent advances in the analysis and numerical simulation of strain localization in inelastic solids. In *Proceedings of the Computational Plasticity*, Owen DRJ, Onate E, Hinton E (eds). vol. IV, CIMNE, Barcelona, Spain, April 1995; 547–561.
26. Oliver J. Continuum modelling of strong discontinuities in solid mechanics. In *Proceedings of the Computational Plasticity*, Owen DRJ, Onate E, Hinton E (eds). vol. IV, CIMNE, Barcelona, Spain, April 1995; 455–479.
27. Larsson R, Runesson K. Element-embedded localization band based on regularized displacement discontinuity. *Journal of Engineering Mechanics* 1996; **122**:402–411.
28. Belytschko T, Lu YY, Gu L. Element-free Galerkin methods. *International Journal for Numerical Methods in Engineering* 1994; **37**:229–256.
29. Belytschko T, Kronggauz Y, Organ D, Fleming M. Meshless methods: an overview and recent developments. *Computer Methods in Applied Mechanics and Engineering* 1996; **139**:3–47.
30. Chen JS, Pan C, Roque C, Wang HP. A Lagrangian reproducing Kernel particle method for metal forming analysis. *Computational Mechanics* 1998; **22**:289–307.
31. Liu WK, Jun S, Zhang YF. Reproducing Kernel particle methods. *International Journal for Numerical Methods in Fluids* 1995; **20**:1081–1106.
32. Liu WK, Chen Y. Wavelet and multiple scale reproducing Kernel particle methods. *International Journal for Numerical Methods in Fluids* 1995; **21**:901–931.

33. Liu WK, Jun S, Li S, Adee J, Belytschko B. Reproducing Kernel particle methods for structural dynamics. *International Journal for Numerical Methods in Engineering* 1995; **38**:1655–1679.
34. Liu WK, Li S, Belytschko T. Moving least square Kernel Galerkin method, Part I. Methodology and convergence. *Computer Methods in Applied Mechanics and Engineering* 1997; **143**:422–433.
35. Lu YY, Belytschko T, Gu L. A new implementation of the element free Galerkin method. *Computer Methods in Applied Mechanics and Engineering* 1994; **113**:397–414.
36. Lancaster P, Salkauskas K. Surfaces generated by moving least squares methods. *Mathematical Computation* 1981; **37**:141–158.
37. Chen JS, Pan C, Wu CT, Liu WK. Reproducing Kernel particle methods for large deformation analysis of nonlinear structures. *Computer Methods in Applied Mechanics and Engineering* 1996; **139**:195–227.
38. Chen JS, Pan C, Wu CT. Large deformation analysis of rubber based on a reproducing Kernel particle method. *Computational Mechanics* 1997; **19**:211–227.
39. Li S, Liu WK. Moving least-squares reproducing Kernel method, Part III: Wavelet packet and its applications. *Computer Methods in Applied Mechanics and Engineering* 1997, submitted for publication.
40. Li S, Liu WK. Synchronized reproducing Kernel interpolant via multiple wavelet expansion. *Computational Mechanics* 1997; **21**:28–47.
41. Chen JS, Wang HP. New boundary condition treatments for meshless computation of contact problems. *Computer Methods in Applied Mechanics and Engineering* 1998, in press.
42. Lemaitre J. A continuous damage mechanics model for ductile fracture. *Journal of Engineering Materials and Technology* 1985; **107**:83–89.
43. Simo JC, Ju JW. Strain- and stress-based continuum damage models-I. Formulation. *International Journal of Solids and Structures* 1987; **23**:821–840.
44. Peerling RHJ, de Borst R, Brekelmans WAM, Vree JHP. Gradient enhanced damage for quasi-brittle materials. *International Journal for Numerical Methods in Engineering* 1996; **39**:3391–3403.
45. Chen JS, Yoon S, Liu WK. An improved reproducing Kernel particle method for nearly incompressible hyperelastic solids. *Computer Methods in Applied Mechanics and Engineering* 1999, in press.
46. Muhlhaus HB, Aifantis EC. A variational principle for gradient plasticity. *International Journal of Solids and Structures* 1991; **28**:845–858.
47. Nayroles B, Tuzot G, Villon P. Generalizing the finite element method: diffuse approximation and diffuse elements. *Computational Mechanics* 1992; **10**:307–318.